Exp Brain Res (2008) 189:311–321
DOI 10.1007/s00221-008-1425-6

RESEARCH ARTICLE

Cortical processing of tactile stimuli applied in quick succession across the fingertips: temporal evolution of dipole sources revealed by magnetoencephalography

Elissaios Karageorgiou · Ioannis G. Koutlas · Aurelio A. Alonso · Arthur C. Leuthold · Scott M. Lewis · Apostolos P. Georgopoulos

Received: 16 January 2008 / Accepted: 7 May 2008 / Published online: 30 May 2008

Abstract We used magnetoencephalography (MEG) in 10 healthy human subjects to study cortical responses to tactile stimuli applied to the fingertips of digits 2–5 of the right hand. Each stimulus lasted 50 ms and was produced by air-driven elastic membranes. Four-hundred stimuli were delivered on each finger in three temporal patterns (conditions). In the "Discrete" condition, stimuli were applied to each finger repetitively with an interstimulus interval (ISI) of 1–2 s. In the "Continuous" condition, stimuli were applied to the fingers sequentially as four-stimulus trains with zero ISI and 1–2 s intervening between trains. Finally, in the "Gap" condition, stimuli were applied as in the Continuous condition but with an ISI of 50 ms. A sensation of tactile motion across fingers (digit 2 → digit 5) was reported by all subjects in the Continuous and Gap conditions. Cortical responses were extracted as single equivalent current dipoles over a period of 1 s following stimulus onset. In all three conditions, initial responses in left primary somatosensory cortex (SI) were observed ~20 to 50 ms after stimulus onset and were followed by additional left SI responses and bilateral responses in the secondary somatosensory cortex (SII). In addition, in the Continuous and Gap conditions, there was an activation of the precentral gyrus, the temporal aspects of which depended on the temporal relation of the administered stimuli, as follows. An ISI of 0 ms led to activation of the precentral gyrus shortly after the second stimulation, whereas an ISI of 50 ms led to activation of the precentral gyrus after the third stimulation. The current findings support results from previous studies on temporal activity patterns in SI and SII, verify the participation of the precentral gyrus during tactile motion perception and, in addition, reveal aspects of integration of sequential sensory stimulations over nonadjacent areas as well as temporal activity patterns in the postcentral and precentral gyri.

E. Karageorgiou · I. G. Koutlas · A. A. Alonso · A. C. Leuthold · S. M. Lewis · A. P. Georgopoulos
Brain Sciences Center, Veterans Affairs Medical Center, Minneapolis, MN 55417, USA

E. Karageorgiou · A. C. Leuthold · A. P. Georgopoulos
Department of Neuroscience, University of Minnesota Medical School, Minneapolis, MN 55455, USA
e-mail: omega@umn.edu

I. G. Koutlas
Department of Diagnostic and Biological Sciences, University of Minnesota School of Dentistry, Minneapolis, MN 55455, USA

A. A. Alonso · A. P. Georgopoulos
Graduate Program in Oral Biology, University of Minnesota, Minneapolis, MN 55455, USA

S. M. Lewis · A. P. Georgopoulos
Department of Neurology, University of Minnesota Medical School, Minneapolis, MN 55455, USA

A. P. Georgopoulos
Department of Psychiatry, University of Minnesota Medical School, Minneapolis, MN 55455, USA

E. Karageorgiou · A. P. Georgopoulos
Center for Cognitive Sciences, University of Minnesota Medical School, Minneapolis, MN 55455, USA

I. G. Koutlas (✉)
Diag/Biolo Sci-Oral Pathology, Room 16-108A Moos T, 515 Delaware St SE, Minneapolis, MN 55455, USA
e-mail: koutl001@umn.edu

Keywords Magnetoencephalography · Dipoles · Somatosensory · Cerebral cortex · Motion perception

Introduction

Magnetoencephalography (MEG) has been developed over the last thirty years as a technique to allow the noninvasive detection of integrated synaptic events (Hämäläinen et al. 1993). MEG has been used successfully not only in the detection of cortical sources of activity but also in calculating the time taken for sensory stimuli to evoke a cortical response, given the superb temporal resolution by which the magnetic signal can be sampled (milliseconds or less). With respect to tactile sensibility, MEG studies in human subjects revealed differential contributions of the primary (SI) and secondary (SII) somatosensory cortices to the somatosensory evoked fields (SEFs) (Hari and Forss 1999; Kakigi et al. 2000). Specifically, it was found that a tactile stimulus in a finger evoked activation of the contralateral SI 20–100 ms after stimulus onset (Hari et al. 1984; Biermann et al. 1998; Hoechstetter et al. 2001). Activation of SII occurred between 45 and 150 ms after stimulus onset (Hoechstetter et al. 2000) with a peak at ~100 ms (Hari and Forss 1999).

Other MEG experiments using finger tactile stimulation have addressed cortical interactions of tactile inputs from adjacent and non-adjacent fingers (Biermann et al. 1998), cortical reorganization after surgical finger separation in syndactyly (Mogilner et al. 1993), investigation of temporal dynamics of activation of SI and SII by simultaneous stimulation to fingers of the same and opposite hands (Hoechstetter et al. 2001), and comparison of the effects of attending to spatial or intensity attributes of a stimulus (Hoechstetter et al. 2000). Finally, cortical activity evoked by a moving tactile stimulus over a contiguous skin surface has also been studied (Cheyne et al. 2003; Lin and Kajola 2003).

Given the existing background, we sought to elucidate the pattern of cortical activity elicited by a non-contiguous stimulation of the skin perceived as tactile motion. To our knowledge, this is the first time that cortical mechanisms underlying motion perception of non-contiguous, yet embryonically related, skin surfaces (adjacent fingertips) are being evaluated. Since this type of experimental design has not been applied before, it was equally possible to observe a pattern of cortical activity similar to those reported in previous experiments based on contiguous skin stimulation, or else a completely novel pattern of activity. Extending the basic experimental plan, we also introduced a temporal delay between sequential finger stimulations while retaining a tactile motion percept. This was done in order to address possible differential processing of tactile motion percepts when the actual motion is not truly continuous.

Specifically, we report on single equivalent current dipole (ECD) analysis of activated cortical areas under three conditions of stimulation of four fingers: (a) individual discrete, (b) continuous sequential and (c) continuous stimulation with an interposed temporal gap. The last two conditions elicited a somatosensory motion percept in all subjects. The purpose of these experiments was to elucidate spatiotemporal cortical activation patterns that arise during perceived tactile motion across fingers, how they resemble and differ relative to discrete tactile stimulation, and how they are affected by manipulating stimulus intervals.

To address these questions we focused on three different analyses relating to different aspects of the information carried by the ECDs. We first evaluated the overall normalized pattern of activation of a given area under a specific condition and whether that would differ across areas or conditions, independent of intensity and fine-temporal differences. Such analysis reveals only the most robust of differences. Subsequently, we focused on finer temporal differences and the first divergence of activity amplitude between areas or conditions. Finally, we evaluated specifically the differences between continuous and gap stimulations as represented in information carried by first-events, given that information is sometimes carried more accurately by first-events (Furukawa and Middlebrooks 2001) rather than general patterns of activity or activity amplitude, aspects of information reflected in the first two analyses.

Materials and methods

Subjects

Ten healthy right-handed subjects (five women, five men; mean ± SEM, 28.4 ± 2.2 years, age range: 18–43 years) participated in the study as paid volunteers. The study protocol was approved by the appropriate institutional review boards and informed consent was obtained from all subjects before the study according to the Declaration of Helsinki.

Stimulus

Subjects rested in a supine position with their eyes closed and their hands at their sides facing upwards. A circular elastic membrane, 1 cm in diameter, was attached to each of the finger pads of fingers 2–5 by a special plastic clamp (Fig. 1). The motion of each membrane was triggered by a computer-generated air pressure stimulus of 17 pounds per square inch. The stimulus lasted 50 ms. There was a delay

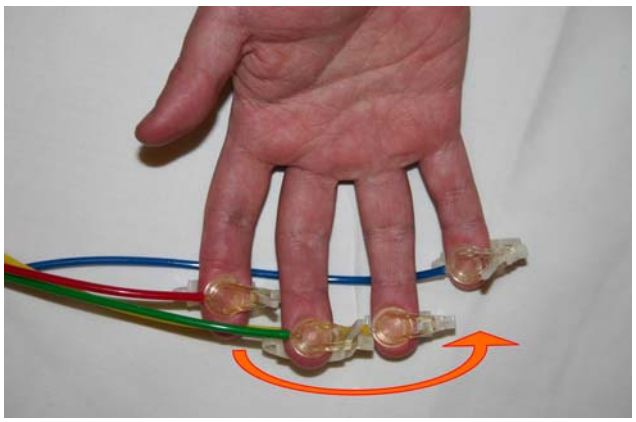

Fig. 1 Air-driven membrane stimulator. The *arrow* represents the sequence of successive stimulations in the Continuous and Gap conditions

of 41 ms from the onset of the trigger to the application of the stimulus (Biermann et al. 1998).

Stimulus delivery

Three different conditions of stimulus delivery were used: (a) discrete individual finger stimulation (Discrete), (b) sequential stimulation of the four fingers with an inter-stimulus interval (ISI) of 0 ms (Continuous), and (c) sequential stimulation of the four fingers with an ISI of 50 ms (Gap). The ISI of 50 ms for the Gap condition was selected, after evaluation of several alternative ISI, to satisfy a single author's perception (ACL) of a continuous motion illusion across fingers without a percept of a temporal gap between different finger stimulations. As such, it was not selected a priori to satisfy a continuous motion percept for all subjects, even though all subjects reported that the sensation was continuous (see Results). For each of the conditions there were 400 repetitions. During the Discrete condition the 400 repetitions were administered on a single finger before stimulating another finger (Fig. 2). A period of 1–2 s was interposed between repetitions.

Data collection

Magnetoencephalography data were collected using a 248-channel axial gradiometer system (Magnes 3600WH; 4D-Neuroimaging, San Diego, USA). The cryogenic helmet-shaped dewar of the MEG was located within an electromagnetically shielded room to reduce noise. Data (0.1–400 Hz) were collected at 1017.25 Hz. For anatomical source localization, T1-weighted gradient-echo images of structural MRI for each subject were acquired (1.5T, SPGR sequence for six subjects; 3T, flash sequence for three subjects; 3T, mprage sequence for one subject).

Data preprocessing and dipole extraction

The acquired time-series data were corrected for the cardiac artifact using event synchronous subtraction (Leuthold 2003). The integrated BESA (v. 5.06, MEGIS Software

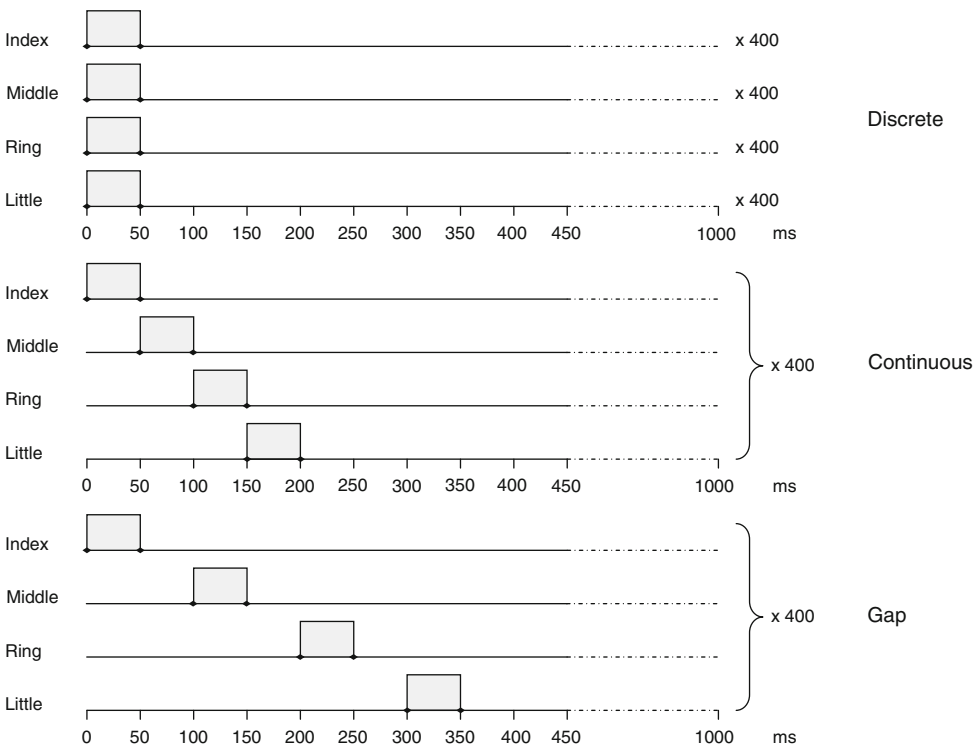

Fig. 2 Temporal patterns of stimulus delivery. *Top* Discrete condition of 400 separate stimulations to each of the four fingers. *Middle* Continuous condition of 400 trains of sequential stimulations to the four fingers with an ISI of 0 ms. *Bottom* Gap condition of 400 trains of sequential stimulations to the four fingers with an ISI of 50 ms

GmbH, Gräfelfing, Germany) BrainVoyager (Electrical Geodesics, Inc, Eugene, OR, USA) package was used for single ECD analysis. Periods of noisy sensors and eye-blink artifacts were manually characterized and eliminated from further analysis. Subsequently, the BESA artifact rejection tool was utilized for more precise artifact characterization (rejecting trials and channels with a range of amplitude >2,000 fT). Epochs were defined from −100 to 1,000 ms from stimulus onset, and a low cutoff filter of 0.1 Hz was used for averaging. The averaged file was then bandpass filtered (high-pass filter: 1 Hz second order; low-pass filter: 44 Hz fourth order; zero-phase). Possible ECD locations with dipolar distribution, and correlated temporal evolution of pole intensity, were determined case-by-case by visual inspection up to 1,000 ms from derived flux maps of sensor waveforms. Only sensors (minimum 12) relevant to these locations were used for further dipole analysis of the respective ECD (Fig. 3). For each subject, the BrainVoyager software was used to create a 3D reconstruction of the brain according to the acquired T1-weighted images. Alignment between the Talairach coordinates of BESA and BrainVoyager was based on fiducials and surface points digitized during acquisition (Langheim et al. 2006).

Using the BESA algorithm for dipole source modeling, ECDs were determined for each of the flux maps and projected onto the 3D-MRI reconstructions of their cortical location (Langheim et al. 2006). Acceptance criteria for ECD localization included (a) goodness of fit of >90%, (b) maximum amplitude of 25 nA, (c) location in cortical gray matter, and (d) duration of ≥10 ms. In waveforms that had multiple peaks, individual peaks were analyzed separately (Fig. 3). The time of occurrence of the peak of each

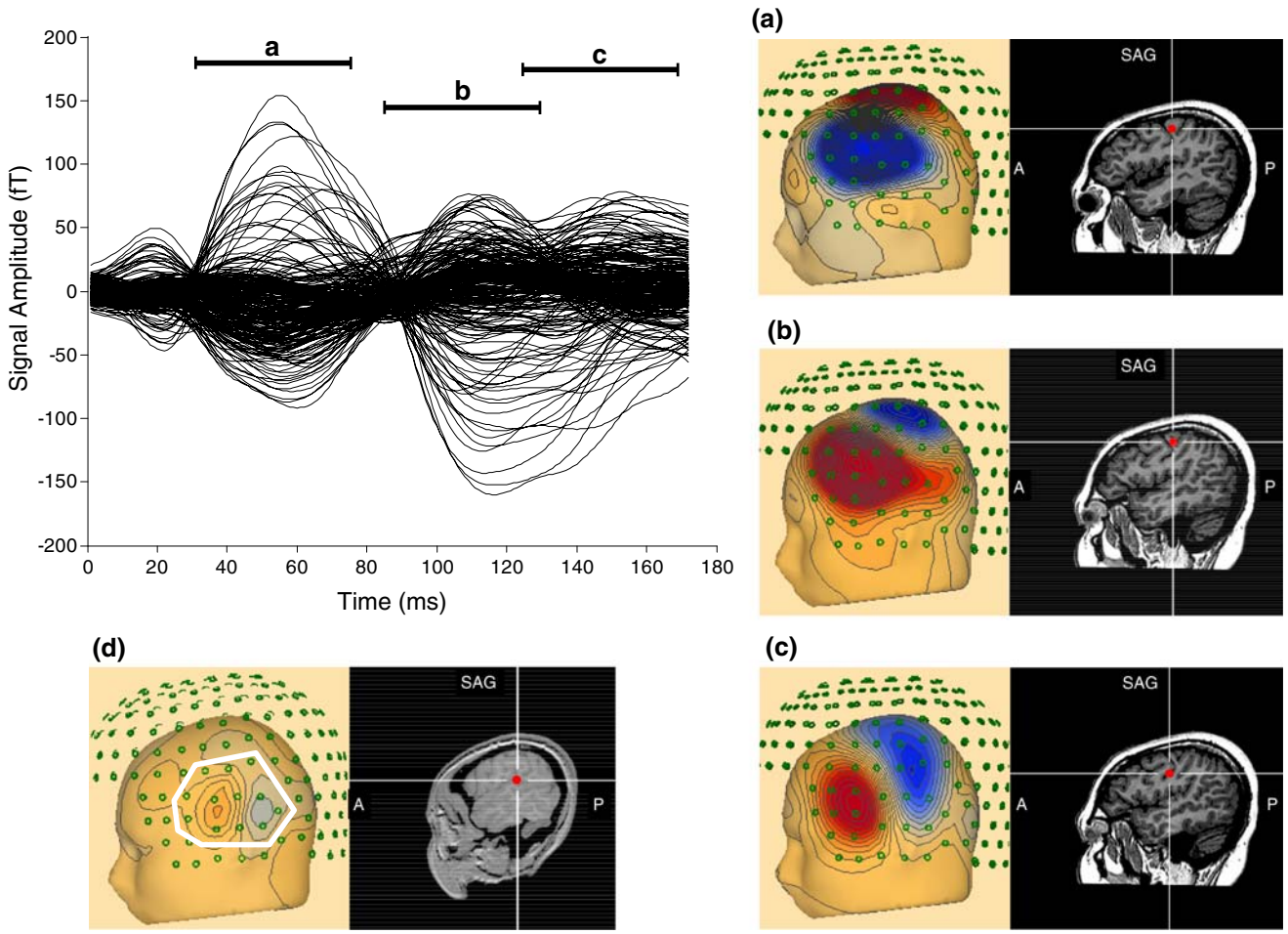

Fig. 3 Dipole source localization. Three ECDs are shown based on a single subject's waveform after stimulation of the index finger. **a** ECD on the postcentral gyrus with a peak at about 55 ms localized using 70 sensors. **b** Recurrent ECD on the postcentral gyrus with a peak at about 110 ms and reversed polarity relative to the previous localized using 66 sensors. **c** ECD in the central sulcus with a peak at about 155 ms and similar polarity to the previous localized using 57 sensors. The last two dipole fields are spatiotemporally overlapping and a selection of a subset of sensors allowed a more accurate characterization of each ECD, additionally avoiding interference from other fields the existence of which can be deduced from the waveform itself. Some of the ECDs were localized using as few as 12 sensors, as shown in **d** for a dipole localized on the supramarginal gyrus of a different subject. Most of these dipoles were observed late (beyond 300 ms) after stimulus onset, and in areas other than the main areas analyzed (see Materials and methods)

derived dipole was noted and was adjusted to account for the transmission delay (41 ms) of the stimulus (air puff) through the tubes.

Assignment to brain areas

The assignment of dipoles to specific regions was based on Talairach coordinates (Talairach and Tournoux 1988) and anatomical landmarks. The following abbreviations are used below: LPoCGy (SI), left postcentral gyrus; LCSul, left central sulcus; LPrCGy, left precentral gyrus; LParOp (SII), left parietal operculum; RParOp (SII), right parietal operculum.

Statistical analyses

The data consisted of the dipole peak latencies (from stimulus application) in a given area. We performed analyses on the data as follows.

Alignment of data according to condition

In order to compare temporal patterns of activity between conditions, two temporally aligned-discrete conditions were simulated from individual finger stimulations, such that stimuli onsets corresponded to those of the Continuous and Gap conditions. Specifically, ECD peak latencies observed during individual finger stimulations were shifted in time according to the finger stimulated and the condition of comparison. For an intuitive understanding, consider in Fig. 2 the individual stimuli at the top panel, and by extension dipole latencies, shifted in a manner to correspond to the middle and bottom panels for the Continuous and Gap conditions, respectively. For example, an ECD peak latency observed at 200 ms after stimulation of the middle finger (second stimulus) was temporally shifted to +50 ms, correcting for continuous stimulation, and +100 ms, correcting for gap stimulation, whereas no correction was made for ECD peaks after index stimulation (first stimulus). These temporal shifts were made to account for any spurious observations related to temporally misaligned stimuli and unrelated to perception. Analyses were performed on the time course of activation in five top ranked areas in dipole numbers (LPoCGy, LCSul, LPrCGy, RParOp, LParOp), as follows.

Analysis of the overall time course

For this analysis, the times of dipole peaks in a given area were collapsed across subjects in a single time course. Then, pairwise differences between areas were assessed using a nonparametric test (Kolmogorov–Smirnov test) and its level of significance adjusted for ten multiple comparisons (all possible comparisons between five areas) using the Bonferroni inequality.

Determination of the onset of significant divergence between activation time courses

In this analysis we sought to determine the time at which time courses of activation diverged significantly between cortical areas. For that purpose we first binned the data every 25 ms (total of 40 bins) and computed fractional intervals per bin for each subject, area and condition (see Taira et al. 1995 for details on calculating fractional intervals). We then applied a sequential t test on the averaged (per subject) fractional interval bins (Armitage 1975) between conditions (for a given area) and between areas (for a given condition), as follows. The standard deviation, σ, of the 40 total bins was then calculated to construct boundaries to test the significance of accumulated changes in differences of activation. For that purpose, a running cumulative sum (CUSUM) was computed of the successive differences between the corresponding (per bin) values of the averaged fractional intervals, starting from the time of stimulus application continuing forward:

$$\mathrm{CUSUM}(n) = \sum_{i=1}^{n} \left(a_i^k - a_i^m\right) \quad (1)$$

where n is the current bin, and a_i^k, a_i^m are the values of fractional intervals in bin i and area (or condition) k and m, respectively. On the null hypothesis that these values do not differ significantly from one another, the value of the CUSUM should tend to be zero. However, fluctuations of the CUSUM above or below zero will occur by chance, and it is the purpose of the sequential procedure to test whether a particular deviation from zero is statistically significant. This was accomplished as follows. Expected chance levels of the CUSUM were calculated for every CUSUM value, that is for every bin contributing a difference to the running CUSUM. Two boundaries were thus generated: an upper (positive) and a lower (negative); when the CUSUM became greater than the upper, or less than the lower boundary, a significant increase or decrease, respectively, in the bin rate was deemed to have occurred, compared to the mean control rate. The boundaries were functions of three variables. The first was the standard deviation σ of the differences being summed. The second factor related to how many times the testing has been performed. It has been shown that the probability that a significant change will be found by chance alone increases as a test of significance is performed repeatedly (see Armitage 1975, pp 27–31). Therefore, for proper sequential (or repeated) testing, the boundaries will have to expand as the bin number increases. Finally, the third factor related to the level of the significance testing desired (e.g., 5 or 1%), the critical value of

change to be detected, and the statistical plan involved. Now, there are basically two kinds of plans: open and closed. In the open plans, repeated testing can continue indefinitely; for this reason they are inappropriate for our application, because our data were of finite length. Closed plans involve repeated testing for a certain number of times, depending on the extent of the data available and on the critical difference to be detected. Closed, restricted plans with known variability were used in the present analysis.

The following equations for the upper (U) and lower (L) boundaries were used (Armitage 1975, p. 97):

$$U : y = 5.2\sigma + 0.35\sigma n$$
$$L : y = -5.2\sigma - 0.35\sigma n$$

where σ was as defined above and n is the bin number, being incremented from the time of stimulus application. The constants 5.2 and 0.35 relate to the plan, the significance level chosen, and the number of repeated tests allowed: they correspond to a closed, restricted plan with two-sided overall significance level, $2\alpha = 0.033$; power, $1\text{-}ß = 0.95$; critical value of change to be detected, $\delta_1 = 0.7$; and an approximate maximum of 36 times of testing (see Table 5.3 in Armitage 1975, p. 101). Although we had 40 bins in our sample, the Table above gave constants for 36 or 49 trials, of which we chose 36, which were closer to our bin number and also more conservative. The testing was stopped when either boundary was crossed by the CUSUM or the last bin reached without crossing.

First-dipole analysis

In this analysis we compared the onset times of the first dipole (from stimulus onset) between the Continuous and Gap conditions in each area using paired t test.

Results

All subjects reported a tactile motion percept during sequential stimulation (Continuous and Gap), in contrast to individual discrete stimuli applied on a single finger which elicited a discrete sensory percept. Regarding brain activity, at least one ECD was found in 36 areas, in both hemispheres. The five top ranked areas in dipole numbers were LPoCGy, LCSul, LPrCGy, RParOp and LParOp. Detailed quantitative analyses were performed on these areas with the following results.

Temporal activity patterns: overall time course

Discrete condition

In this analysis, the overall time course (over 1 s following stimulus application) was compared between areas using the Kolmogorov–Smirnov test. ECDs appeared in left SI (LPoCGy) shortly after stimulus onset, at ~40 to 50 ms in all subjects; there was an additional earlier activation at ~20 ms in three subjects. (In subjects where an early 20 ms ECD was not observed, we examined sensor waveforms and identified a very weak SEF component.) A later, recurrent activation was also observed following the primary sensory dipoles (Fig. 4). This pattern of activation was very similar for all fingers and did not differ significantly among them (Fig. 5; $P > 0.8$ for all pairwise comparisons, Kolmogorov–Smirnov test).

In the LCSul, ECDs also appeared shortly after stimulus onset in each condition, at ~40 to 50 ms in all subjects. A later, recurrent activation was observed following the primary sensory dipoles (Fig. 6). In contrast, only two subjects showed ECDs in LPrCGy, which clustered in two peaks, centered at 50 and 270 ms after stimulus onset.

Bilateral activation of SII (ParOp) followed shortly after SI at approximately 60 to 110 ms. Specifically, in left SII (LParOp), ECDs were inconsistent (e.g., observed mainly after little finger stimulation) and mostly occurred up to 150 ms. In contrast, the right SII (RParOp) was consistently activated in all subjects and fingers. There were three decrementing ECD clusters (Fig. 7), at 50–200, 250–400, and 500–600 ms.

Continuous and Gap conditions

Equivalent current dipoles appeared in left SI shortly after stimulus onset, at ~40 to 50 ms in all subjects. Recurrent activation was also observed following the primary sensory dipoles and extended well up to 600–650 ms in a prominent, yet decrementing, manner. This pattern of overall

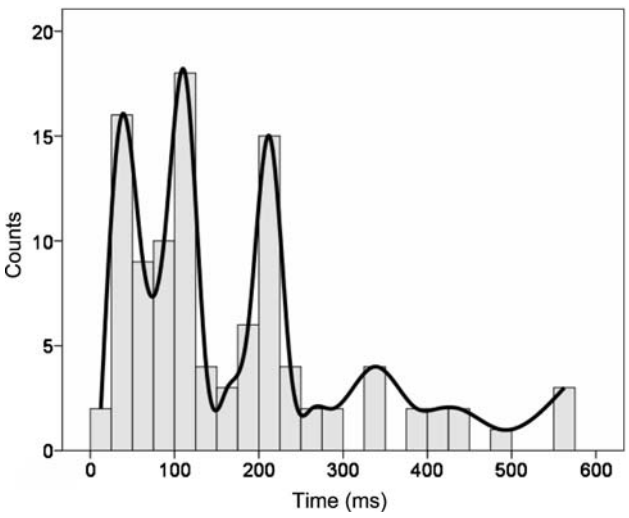

Fig. 4 Histogram of ECD activity in SI during the Discrete condition with 25 ms bins. An initial peak is observed at 25–50 ms with recurrent ECDs peaking at 100–125 and 200–225 ms

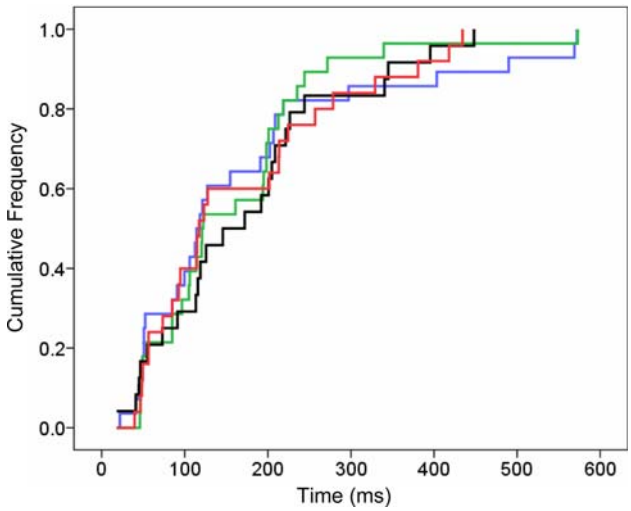

Fig. 5 Cumulative frequency curves for each of the four fingers during the Discrete condition. *Blue* Index, *green* middle, *black* ring, *red little*. No significant difference was observed between any of the individual finger ECD overall activity (Kolmogorov–Smirnov, $P > 0.8$)

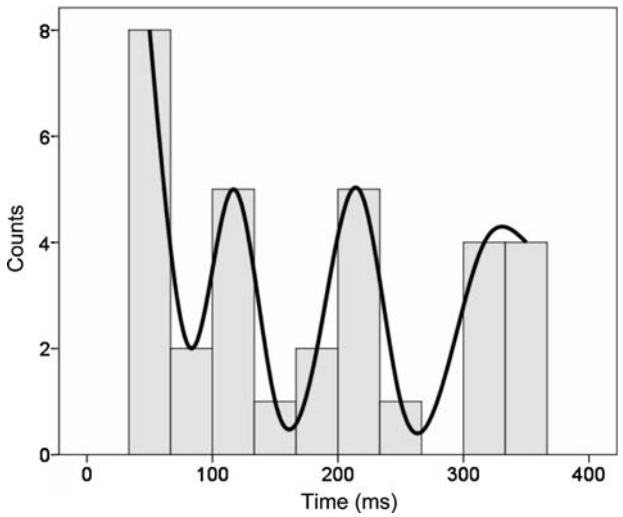

Fig. 6 Histogram of ECD activity in LCSul during the Discrete condition with 33 ms bins. An initial peak is observed at 33–66 ms with recurrent ECDs peaking at 100–133, 200–233 and 300–366 ms

activation did not differ significantly between the Continuous and Gap condition ($P = 0.972$, Kolmogorov–Smirnov test).

Equivalent current dipoles activation in LCSul began at ~40 to 50 ms in both Continuous and Gap conditions and did not differ significantly between the two conditions ($P = 0.555$ Kolmogorov–Smirnov test).

In LPrCGy, clear activation occurred consistently in both Continuous and Gap conditions (Fig. 8), in contrast to the inconsistent activation observed in the Discrete condition (see above). The earliest ECD in the Continuous condition preceded that in the Gap condition by ~100 ms.

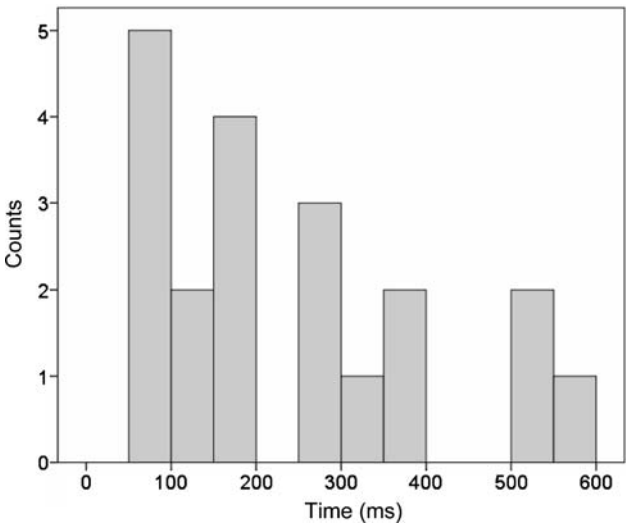

Fig. 7 Histogram of ECD activity in right SII during the Discrete condition with 50 ms bins. ECD activity is clustered between 50–200, 250–400 and 500–600 ms

In the Continuous condition ECDs were clustered at ~100 ms post stimulus onset, whereas in the Gap condition at ~400 ms. However, the overall ECD distribution for the two conditions was marginally non-significant ($P = 0.057$, Kolmogorov–Smirnov test).

Bilateral activation of SII was also observed in the Continuous and the Gap conditions. As in the Discrete condition, LParOp showed inconsistent activation. In contrast, activation of RParOp began at ~50 ms following stimulus

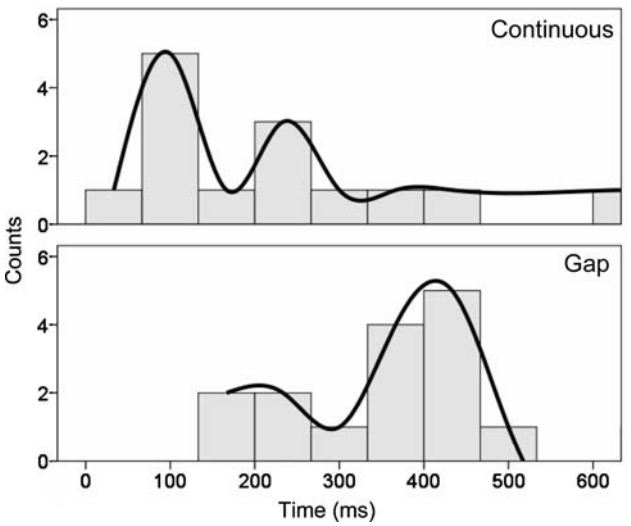

Fig. 8 Histogram of ECD activity in LPrCGy during the Continuous (*top*) and Gap (*bottom*) conditions with 66 ms bins. First-dipole latencies were shorter during the Continuous compared to the Gap condition (paired *t* test, $P = 0.041$). Additionally, ECDs peaked early after second finger stimulation (~100 ms) in the Continuous condition, whereas after the third and even fourth finger stimulations (~400 ms) in the Gap condition (compare to Fig. 2)

application and extended up to ~250 ms; the time course of ECD activation did not differ significantly between the two conditions ($P = 0.893$ Kolmogorov–Smirnov test).

Finally, the time courses for the Discrete condition (aligned accordingly, see Materials and methods) did not differ significantly from those for the Continuous and Gap condition in any of the above areas (Kolmogorov–Smirnov test). (For LPrCGy this could not be tested due to its inconsistent activation in the Discrete condition, see above.)

Comparison between areas

We found that the overall time course in the Discrete condition did not differ significantly between any areas. No significant differences were found between any areas for the Continuous or the Gap conditions.

Temporal divergence of activation

In this analysis we determined the earliest time of statistically significant divergence of time course using fractional intervals (see Materials and methods). This analysis compares the temporal evolution of intensity of activation, in contrast to the one in the preceding section which compares normalized overall time courses.

Tests between areas for each condition

For the Discrete condition, we found the following: (a) LPoCGy was activated more than any other area (LCSul, LPrCGy, LParOp, RParOp), beginning at the second time bin (25–50 ms) after stimulus application. (b) LCSul was activated more than LPrCGy, LParOp, and RParOp, also at 25–50 ms. (c) LPrCGy was activated more than LParOp at 25–50 ms, whereas no difference was found with respect to RParOp. Finally, (d) RParOp was more highly activated than LParOp, starting at 50–75 ms.

For the Continuous condition, we found the following. (a) LPoCGy was activated more than any other area (LCSul, LPrCGy, LParOp, RParOp), beginning at the second time bin (25–50 ms) after stimulus application. (b) LCSul was activated more than LParOp and RParOp at 25–50 ms, whereas no significant divergence was identified between the time courses of LCSul and LPrCGy. (c) LPrCGy was activated more than LParOp and RParOp at 25–50 ms. Finally (d) RParOp was more highly activated than LParOp, at 25–50 ms.

Finally, for the Gap condition, we found the following. (a) LPoCGy was activated more than any other area (LCSul, LPrCGy, LParOp, RParOp), beginning at the second time bin (25–50 ms) after stimulus application. (b) LCSul was activated more than LParOp and RParOp at 25–50 ms. (c) LPrCGy was activated more than LCSul (at 425–450 ms), LParOp (at 150–175 ms), and RParOp (at 275–300 ms). Finally, (d) RParOp was more highly activated than LParOp, at 50–75 ms.

Tests between conditions for each area

For left SI, we found the following. (a) There was more activity in the Discrete versus Continuous condition, beginning at the 4th time bin (75–100 ms) after stimulus application. (b) There was no significant divergence in the time courses of Discrete and Gap conditions. Finally, (c) there was more activity in the Gap versus Continuous condition, starting at the fourth time bin (75–100 ms) (Fig. 9).

For the LCSul, we found the following. (a) There was no significant divergence in the time course between the Discrete versus Continuous condition. (b) There was more activity in the Discrete versus Gap condition, starting at the ninth bin (200–225 ms). Finally (c) there was more activity in the Continuous versus Gap, starting at the first time bin (25 ms).

For the LPrCGy, we found the following. (a) There was more activity in the Continuous versus Discrete condition, starting at the second time bin (25–50 ms). (b) There was more activity in the Gap versus Discrete condition, starting at the 11th bin (250–275 ms). Finally, (c) there was more activity in the Continuous versus Gap, starting at the fourth time bin (75–100 ms) (Fig. 10).

For the ParOp we found the following. (a) There was more activity starting at the fifth time bin (100–125 ms) in the RParOp, and less activity starting at the sixth time bin (125–150 ms) in the LParOp during the Gap versus Continuous condition. (b) There was less activity in the Gap

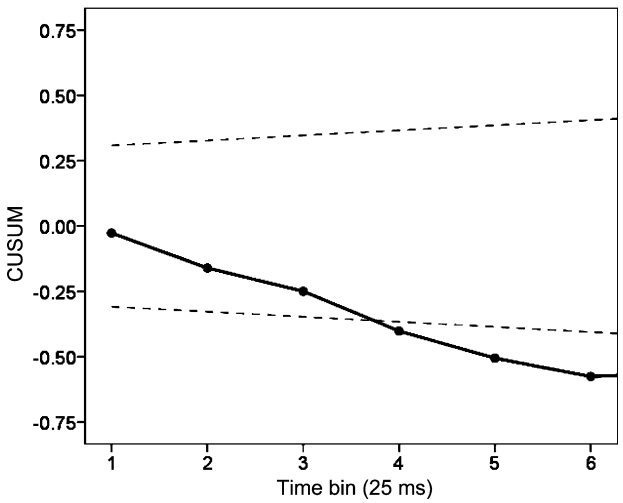

Fig. 9 Divergence of activity through fractional interval in left SI comparing continous versus Gap conditions. The first divergence of activity is in favor of the Gap condition starting at the fourth time bin (75–100 ms)

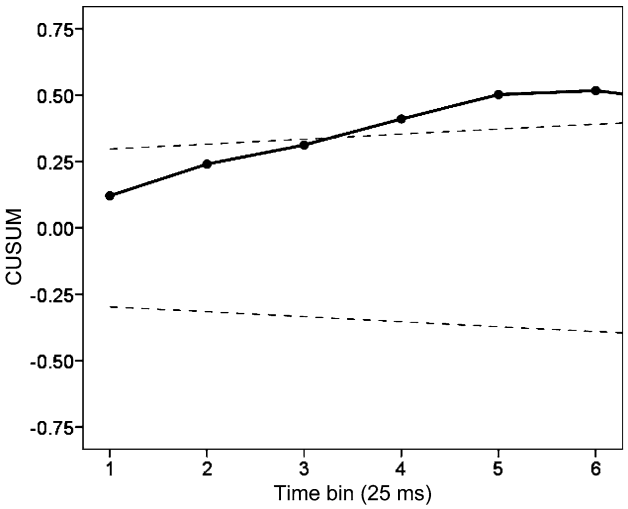

Fig. 10 Divergence of activity through fractional interval in LPrCGy comparing continous versus Gap conditions. The first divergence of activity is in favor of the Continuous condition starting at the fourth time bin (75–100 ms)

versus Discrete condition starting at the 13th time bin (300–325 ms) in the RParOp, and at the 15th time bin (350–375 ms) in the LParOp. (c) There was more activity in the Continuous versus Discrete condition at the 4th time bin (75–100 ms) in the LParOp, and less activity starting at the 8th time bin (175–200 ms) in the RParOp.

First-dipole analysis

This analysis revealed differences between the Continuous and Gap conditions with respect to the latency of the first dipole from stimulus onset. Given the analogy of our data to single-events, we followed a first-event approach already applied on spike data in neurophysiological experiments successfully (Schmolesky et al. 1998), and in some cases even more than the overall event count (Furukawa and Middlebrooks 2001). Moreover, specifically for somatosensory stimuli, disruption of the temporal pattern of activation has been shown to result in a reduction in the conveyed information (Ghazanfar et al. 2000).

In our data, the only area with a significant difference in first-dipole latency between the Continuous and Gap conditions was the LPrCGy ($P = 0.041$, paired t test), with the first-dipole occurring 186.6 ± 68.3 ms earlier in the Continuous relative to the Gap condition. No significant differences were found in any other area.

Discussion

In this study we sought to elucidate the cortical spatio-temporal patterns elicited by the application in quick succession of stimuli across fingers. Such stimuli elicited a tactile motion percept, in contrast to single, discrete stimuli applied on a single finger which elicit a discrete sensory percept. In all conditions, discrete and sequential, the stimulus elicited a response in contralateral SI, followed by recurrent SI responses and bilateral SII responses. However, sequential stimulation activated preferentially the precentral gyrus; this activation was much earlier when there was no temporal gap between the stimuli applied. Overall, these results are in keeping with previous findings of MEG studies of SEF of primary sensory responses (Hari and Forss 1999; Kakigi et al. 2000), feedback activation of SI based on neurophysiological experiments (Gibson et al. 1999; Ahissar and Kleinfeld 2003; Kleinfeld et al. 2006), and on localizing cortical activity during tactile motion perception from fMRI studies (Bremmer et al. 2001).

Sensory areas involved in tactile motion stimulation

SI was activated shortly (40–50 ms) after stimulus onset in each condition and in all subjects. Bilateral activation of SII (ParOp) followed at approximately 60–110 ms. These results are in accord with previous studies (Hari and Forss 1999; Hoechstetter et al. 2000). In experiments where data were analyzed using SEFs (Kaufman et al. 1981; Hari et al. 1984), sensory responses extended over a period of 20–250 ms, with a first component at ~20 ms and a stronger second component at ~50 ms (Hari and Forss 1999). Only three subjects from our study had ECDs in SI detected as early as 20 ms (corresponding, thus, to the first SEF component). However, all subjects showed ECD activity between 40 and 50 ms which reflects the second component in SEFs. The fact that ECDs always reflected the second SEF component is in accord with results from other studies evaluating dipole activity (Mogilner et al. 1993; Biermann et al. 1998).

Beyond primary sensory responses, we also observed recurrent SI activation (Fig. 4), which indicates additional tactile sensory processing. The recurrent SI activation after discrete stimulation is in keeping with results of neurophysiological studies of SI and motor cortex in animals (Stefanis and Jasper 1964a, b; Ahissar and Kleinfeld 2003; Kleinfeld et al. 2006). In addition, a balance between excitatory and inhibitory pathways has been proposed where feed-forward thalamocortical and local recurrent circuits cooperate for synchronous firing in SI (Miller et al. 2001), synchronicity being a prerequisite in MEG source detection (Hämäläinen et al. 1993). Local cortical synchronization may thus rely on recurrent collaterals of pyramidal tract cells (Stefanis and Jasper 1964a, b), specific parvalbumin-immunoreactive thalamocortical neurons (Jones 2001) and fast-spiking inhibitory cortical interneurons receiving thalamic input (Gibson et al. 1999). The

decline over time of the number of recurrent ECDs can be explained as a decay in the driving thalamocortical input leading to desynchronization and dampening of the cortical signal. This pattern of recurrent SI activation can also explain the divergence in ECD activity during the Continuous condition as compared to the Gap (Fig. 9) and the Discrete conditions, as follows. The first recurrent ECDs during the Gap condition were observed between primary sensory ECDs (from each finger) with which they did not overlap, whereas during the Continuous condition this overlap is inevitable. Similarly, recurrent ECDs during the Discrete condition are always observed.

In addition to SI activation, Bremmer et al. (2001) have shown that SII is bilaterally involved in tactile motion perception during stimulation of adjacent skin areas using fMRI. In that study, moving stimuli were applied on the forehead, in contrast to the present study in which discrete stimuli (on adjacent fingers) were applied in quick succession; in both cases, a tactile motion was perceived. In the fMRI study, a bilateral activation of SII was found but its time course could not be determined, given the TR time of 5 s used. In this study, we were able to analyze the time course of activation in fine detail, given the high-temporal resolution of MEG, and found a diverging activity between stimulus conditions in both the left and right SII (ParOp), as follows. In RParOp, the first significant divergence in the time course of activity was highest in the Discrete condition, whereas in LParOp it was highest in the Continuous condition. This finding suggests that LParOp might be preferentially involved in tactile motion illusion.

Precentral gyrus in tactile motion stimulation

The most interesting findings in the current analysis relate to activity patterns of the LPrCGy. Previous studies using fMRI have revealed increased activity in precentral areas during tactile motion perception while stimulating the forehead (see Fig. 1b in Bremmer et al. 2001; Soto-Faraco et al. 2004). A reasonable doubt in MEG experiments using tactile stimulation is whether ECDs detected on the LPrCGy area could be the result of a modeling error from SI activity (Huttunen 1997). If that were the case, the pattern of ECD activity in the LPrCGy in our experiment should be comparable to that of SI. However, this was not observed. Specifically, there was only sparse involvement of LPrCGy in the Discrete condition but much more substantial involvement during the Continuous and Gap conditions. This finding suggests that precentral activity might subserve a higher-order, common (i.e., including Continuous and Gap stimulation) tactile motion percept.

Now, with respect to differences in the activation of LPrCGy between the Continuous and Gap conditions it was marginally non-significant ($P = 0.057$). Significant differences between the two conditions were firmly established when looking at the time period when LPrCGy activity increased. A first observation related to the peak of ECD activity which was between 66 and 133 ms in the Continuous condition, and between 400 and 466 ms in the Gap condition (Fig. 8). In addition, since there were ECDs in the Gap condition observed as early as 133–200 ms and given the information conveyed in first-events (Schmolesky et al. 1998; Ghazanfar et al. 2000; Furukawa and Middlebrooks 2001; Johansson and Birznieks 2004), we evaluated whether there was a true difference in first-dipole latency between the two conditions. Indeed, the LPrCGy revealed a consistent earlier activation by approximately 187 ms during the Continuous compared to the Gap condition. A third difference in the temporal evolution of ECD activity between the two conditions was the onset of divergence as expressed by the CUSUM, which started at 75–100 ms post stimulus onset.

Combining the above observations on described differences in latency, divergence and peak ECD activity, there is a robust difference in how stimuli in the Continuous and Gap conditions are processed in the LPrCGy. Specifically, stimulation of the first two fingers is enough to elicit a substantial LPrCGy response during the Continuous condition, whereas during the Gap condition a third and probably a fourth finger stimulation is required to elicit a comparable response (compare Figs. 2 and 8 for stimulation alignment, see Materials and methods). If we suppose that the presence of LPrCGy activation underlies a tactile motion percept, then the findings above predict that for such a percept to be elicited in the Gap condition, at least a third, and possibly a fourth stimulus is needed. This hypothesis remains to be tested.

Additional findings

It is worth noting that a substantial amount of total activity was found in LCSul in all conditions and with a pattern of activity similar, although not as strong, to that observed in SI (Fig. 6). Based on this similarity to SI activity, dipoles from LCSul probably pertain to simple tactile sensory responses, a finding consistent with neurophysiological experiments (Kaas et al. 1979). However, because these responses were elicited on the border between the two main areas of interest (postcentral and precentral), they were analyzed separately. Regarding the rest of the areas, the bilateral activation of ParOp (SII) supports previous MEG data based on tactile stimulation (Hari and Forss 1999; Hoechstetter et al. 2000). Also, the fact that the activity of the LParOp was inconsistent and less than that of the right parietal operculum could be attributed to a masking of dipoles in SII by the recurrent activity in the overlying SI. This hypothesis could not be tested directly with the single

dipole analysis used in this study. Finally, both the Continuous (ISI = 0 ms) and Gap (ISI = 50 ms) conditions elicited a tactile motion percept. A detailed, quantitative study of the subjects' psychophysical rating of motion perception in relation to brain activity remains to be done.

Acknowledgments This work was supported by a Grant-In-Aid Program, Graduate School, University of Minnesota, to I. G. Koutlas, the Department of Veterans Affairs, and the American Legion Brain Sciences Chair.

References

Ahissar E, Kleinfeld D (2003) Closed-loop neuronal computations: focus on vibrissa somatosensation in rat. Cereb Cortex 13:53–62

Armitage P (1975) Sequential medical trials. Wiley, New York

Biermann K, Schmitz F, Wittee OW, Konczak J, Freund H-J, Schnitzler A (1998) Interaction of finger representation in the human first somatosensory cortex: a neuromagnetic study. Neurosci Lett 251:13–16

Bremmer F, Schlack A, Shah NJ, Zafiris O, Kubischik M, Hoffmann K, Zilles K, Fink GR (2001) Polymodal motion processing in posterior parietal and premotor cortex: a human fMRI study strongly implies equivalencies between humans and monkeys. Neuron 29:287–296

Cheyne D, Gaetz W, Garnero L, Lachaux J-P, Ducorps A, Schwartz D, Varela FJ (2003) Neuromagnetic imaging of cortical accompanying tactile stimulation. Cogn Brain Res 17:599–611

Furukawa S, Middlebrooks JC (2001) Cortical representation of auditory space: Information-bearing features of spike patterns. J Neurophysiol 87:1749–1762

Ghazanfar AA, Stambaugh CR, Nicolelis MA (2000) Encoding of tactile stimulus location by somatosensory thalamocortical ensembles. J Neurosci 20:3761–3775

Gibson JR, Beierlein M, Connors BW (1999) Two networks of electrically coupled inhibitory neurons in neocortex. Nature 402:75–79

Hämäläinen M, Hari R, Ilmoniemi R, Knuutila J, Lounasmaa OV (1993) Magnetoencephalography—theory, instrumentation, and applications to noninvasive studies of signal processing in the human brain. Rev Modern Phys 65:413–497

Hari R, Reinikainen K, Kaukoranta E, Hämäläinen M, Ilmoniemi R, Penttinen A, Salminen J, Teszner D (1984) Somatosensory evoked cerebral magnetic fields from SI and SII in man. Electroencephalogr Clin Neurophysiol 57:254–263

Hari R, Forss N (1999) Magnetoencephalography in the study of human somatosensory cortical processing. Philos Trans R Soc Lond B Biol Sci 354:1145–1154

Hoechstetter K, Rupp A, Stančák A, Meinck H-M, Weckesser D, Bornfleth H, Stippich C, Berg P, Scherg M (2000) Magnetic source imaging of tactile input shows task-independent attention effects in SII. NeuroReport 11:2461–2465

Hoechstetter K, Rupp A, Stančák A, Meinck H-M, Stippich C, Berg P, Scherg M (2001) Interaction of tactile input in the human primary and secondary somatosensory cortex—a Magnetoencephalographic study. NeuroImage 14:759–767

Huttunen J (1997) Does the P35m SEF deflection really come from the motor cortex? Electroencephalogr Clin Neurophysiol 104:101–102

Johansson RS, Birznieks I (2004) First spikes in ensembles of human tactile afferents code complex spatial fingertip events. Nat Neurosci 7:170–177

Jones EG (2001) The thalamic matrix and thalamocortical synchrony. Trends Neurosci 24:595–601

Kaas JH, Nelson RJ, Sur M, Lin CS, Merzenich MM (1979) Multiple representations of the body within the primary somatosensory cortex of primates. Science 204:521–523

Kakigi R, Hoshiyama M, Shimojo M, Naka D, Yamasaki H, Watanabe S, Xiang J, Maeda K, Lam K, Itomi K, Nakamura A (2000) The somatosensory evoked magnetic fields. Prog Neurobiol 61:495–523

Kaufman L, Okada Y, Brenner D, Williamson SJ (1981) On the relation between somatic evoked potentials and fields. Int J Neurosci 15:223–239

Kleinfeld D, Ahissar E, Diamond ME (2006) Active sensation: insights from the rodent vibrissa sensorimotor system. Curr Opin Neurobiol 16:435–444

Langheim FJP, Merkle AN, Leuthold AC, Lewis SM, Georgopoulos AP (2006) Dipole analysis of magnetoencephalographic data during continuous shape copying. Exp Brain Res 170:513–521

Leuthold AC (2003) Subtraction of heart artifact from MEG data: the matched filter revisited. Society for Neuroscience Abstracts 863.15

Lin YY, Kajola M (2003) Neuromagnetic somatosensory responses to natural moving tactile stimulation. Can J Neurol Sci 30:31–35

Miller KD, Pinto DJ, Simons DJ (2001) Processing in layer 4 of the neocortical circuit: new insights from visual and somatosensory cortex. Curr Opin Neurobiol 11:488–497

Mogilner A, Grossman JA, Ribary U, Joliot M, Volkmann J, Rapaport D, Beasley RW, Llinás RR (1993) Somatosensory cortical plasticity in adult humans revealed by magnetoencephalography. Proc Natl Acad Sci USA 90:3593–3597

Schmolesky MT, Wang Y, Hanes DP, Thompson KG, Leutgeb S, Schall JD, Leventhal AG (1998) Signal timing across the macaque visual system. J Neurophysiol 79:3272–3278

Soto-Faraco S, Spence C, Lloyd D, Kingstone A (2004) Moving multisensory research along: motion perception across sensory modalities. Curr Direct Psychol Sci 13:29–32

Stefanis C, Jasper H (1964a) Intracellular microelectrode studies of antidromic responses in cortical pyramidal tract neurons. J Neurophysiol 27:828–854

Stefanis C, Jasper H (1964b) Recurrent collateral inhibition in pyramidal tract neurons. J Neurophysiol 27:855–877

Taira M, Boline J, Smyrnis N, Georgopoulos AP, Ashe J (1995) On the relations between single cell activity in the motor cortex and the direction and magnitude of three-dimensional static isometric force. Exp Brain Res 109:367–376

Talairach J, Tournoux P (1988) Co-planar stereotaxic atlas of the human brain. Thieme Medical Publishers, New York